Global superdiffusion of weak chaos

Itzhack Dana
Minerva Center and Department of Physics, Bar-Ilan University, Ramat-Gan 52900, Israel
(Received 15 April 2003; revised manuscript received 4 September 2003; published 29 January 2004)

A class of kicked rotors is introduced, exhibiting accelerator-mode islands (AIs) and *global* superdiffusion for *arbitrarily weak* chaos. The corresponding standard maps are shown to be exactly related to generalized web maps taken modulo an ''oblique cylinder.'' Then, in a case that the web-map orbit structure is periodic in the phase plane, the AIs are essentially *normal* web islands folded back into the cylinder. As a consequence, chaotic orbits sticking around the AI boundary are accelerated *only* when they traverse tiny ''*acceleration spots*.'' This leads to chaotic flights having a quasiregular *steplike* structure. The global weak-chaos superdiffusion is thus basically different in nature from the strong-chaos one in the usual standard and web maps.

DOI: 10.1103/PhysRevE.69.016212 PACS number(s): 05.45.Mt, 05.45.Ac, 45.05.+x

The complexity and rich variety of dynamical behaviors of Hamiltonian systems with two degrees of freedom is well exhibited by simple one-dimensional time-periodic models. A realistic paradigm is the kicked rotor with Hamiltonian $H=p^2/2+V(x)\Sigma_{n=-\infty}^{\infty}\delta(t-n)$, where p is angular momentum, x is angle on a circle $\mathcal{S}=[-\pi,\pi)$, and the potential $V(x)$ is usually chosen as $V(x)=\kappa\cos x$, κ being a nonintegrability parameter. The phase space is a cylinder and the values of $(x,\ p)$ at integer times $t=n-0$ are related by the ''standard'' map [1,2]

$$\mathbf{\Phi}_{\mathrm{s}}:\ p_{n+1}=p_n+f(x_n),\quad x_{n+1}=x_n+p_{n+1}\ \mathrm{mod}\ \mathcal{S}, \quad (1)$$

where $f(x)=-dV/dx=\kappa\sin x$. For $\kappa>\kappa_{\mathrm{c}}\approx 0.9716$, this map features *global* chaos, i.e., a connected chaotic region unbounded in the p direction and ranging from $x=-\pi$ to $x=\pi$ [2]. The average kinetic energy of an ensemble in this region grows diffusively, $\langle p_n^2/2\rangle\propto n$ [1]. For κ significantly larger than κ_{c} (strong-chaos regime), there emerge accelerator-mode islands (AIs) [3–5] moving ballistically $(p_n\propto n)$. Then, chaotic orbits sticking around the boundary of an AI perform also ballistic motion. This leads to long chaotic *''flights''* and to *superdiffusion* of the global chaos, $\langle p_n^2/2\rangle\propto n^{\mu}$ $(1<\mu<2)$ [3,5].

In this paper, we introduce a class of kicked rotors exhibiting AIs and global superdiffusion for *arbitrarily weak* chaos. These systems correspond to standard maps (1) with

$$f(x)=Ks(x)+\kappa g(x), \quad (2)$$

where $-4<K<-2$, κ is a perturbation parameter, $s(x)$ is the sawtooth function $[s(x)=x$ for $x\in\mathcal{S}$ and $s(x+2\pi)=s(x)]$, and $g(x)$ is a general smooth 2π-periodic function. We denote these maps, for $-4<K<0$, by $\mathbf{\Phi}_{\mathrm{s}}^{(K,\kappa)}$. For $\kappa=0$, $\mathbf{\Phi}_{\mathrm{s}}^{(K,0)}$ exhibits generically a pseudochaotic behavior (zero Lyapunov exponent) [6]; important exceptions, with regular elliptic motion, are the cases of integer $K=-3,-2,-1$ [7]. For small κ, weak chaos emerges, see Fig. 1. The superdiffusion for $-4<K<-2$ is usually characterized by large values of μ (for $\kappa=0$, $\mu\approx\mu_{\max}=2$). To get a better understanding of the nature of the AIs and the chaotic flights responsible for the superdiffusion, we first show that $\mathbf{\Phi}_{\mathrm{s}}^{(K,\kappa)}$ is exactly related to a ''web map'' [8,9] taken modulo an ''oblique cylinder.'' A generalized web map $\mathbf{\Phi}_{\mathrm{w}}$ on a phase plane $\mathbf{w}\equiv(u,v)$ (column vector) is defined by

$$\mathbf{\Phi}_{\mathrm{w}}:\ \mathbf{w}_{n+1}=A\cdot[\mathbf{w}_n+\mathbf{F}(\mathbf{w}_n)], \quad (3)$$

where $A=(\cos\alpha,\sin\alpha;-\sin\alpha,\cos\alpha)$ is the matrix for a rotation by angle α and $\mathbf{F}(\mathbf{w})$ is a vector function periodic in $\mathbf{w}$. For integer K, the orbit structure of $\mathbf{\Phi}_{\mathrm{w}}$ is periodic in the phase plane. Then, the AIs of $\mathbf{\Phi}_{\mathrm{s}}^{(K,\kappa)}$ for $K=-3$ are essentially *normal* (nonaccelerating) islands of $\mathbf{\Phi}_{\mathrm{w}}$ folded back into the cylinder. This fact makes these AIs basically different from usual AIs [4] and has a significant impact on the nature of the chaotic flights, as we show by studying in detail the case of $K=-3$ with $g(x)=\sin x$. While elliptic orbits deep inside an AI move ballistically, chaotic orbits sticking to the AI boundary perform ballistic motion *only* when they pass through very small regions which we call ''*acceleration spots*.'' The rest (the majority) of the AI boundary behaves like that of a normal island, so that the chaotic orbits perform a completely *bounded* motion on it. This gives rise to chaotic flights having a quasiregular *steplike* structure which becomes increasingly pronounced as $\kappa\to 0$.

To establish the relation between $\mathbf{\Phi}_{\mathrm{s}}^{(K,\kappa)}$ and $\mathbf{\Phi}_{\mathrm{w}}$, consider first a map $\mathbf{\Psi}^{(K,\kappa)}$ obtained from Eq. (1) by removing the mod $\mathcal{S}$ and by using (2) with $s(x)$ replaced by x. This map, defined on the entire phase plane of $\mathbf{z}\equiv(x,\ p)$, can be written as follows:

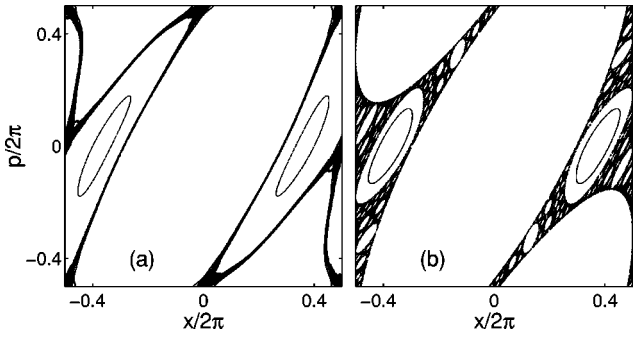

FIG. 1. Global chaos for the standard map (1) with Eq. (2), $g(x)=\sin x$, and (a) $K=-3$, $\kappa=0.8$; (b) $K=-2.724\,749\,8$, $\kappa=0.15$. The AIs are the regions indicated by elliptic orbits.

$$\mathbf{\Psi}^{(K,\kappa)}\colon\ \mathbf{z}_{n+1}=B\cdot[\mathbf{z}_n+\mathbf{G}(\mathbf{z}_n)], \tag{4}$$

where B is the matrix $(K+1,1;K,1)$ and $\mathbf{G}(\mathbf{z})=\kappa g(x)\times(0,1)$. For $-4<K<0$, one can easily verify that $B=Q^{-1}AQ$, where $A=(\cos\alpha,\sin\alpha;-\sin\alpha,\cos\alpha)$ with

$$2\cos\alpha=K+2 \tag{5}$$

and $Q=(k,-k/2;0,1/2)$ with $k\equiv\tan(\alpha/2)$. Thus, the composition $Q\circ\mathbf{\Psi}^{(K,\kappa)}\circ Q^{-1}$ is precisely a web map (3) with $\mathbf{w}=(u,v)=Q\cdot\mathbf{z}$ and $\mathbf{F}(\mathbf{w})=Q\cdot\mathbf{G}(Q^{-1}\cdot\mathbf{w})$. Explicitly, $\mathbf{F}(\mathbf{w})=(\kappa/2)g(v+u/k)(-k,1)$. We denote by $\mathcal{C}=[-\pi,\pi)\times(-\infty,\infty)$ the cylindrical phase space for $\mathbf{\Phi}_{\rm s}^{(K,\kappa)}$ and define $\mathbf{\Psi}_{\mathcal{C}}^{(K,\kappa)}$ as the map (4) with x_{n+1} (in first equation) taken modulo $\mathcal{S}$. Clearly, if we restrict ourselves to initial conditions $\mathbf{z}_0\in\mathcal{C}$, $\mathbf{\Psi}_{\mathcal{C}}^{(K,\kappa)}=\mathbf{\Phi}_{\rm s}^{(K,\kappa)}$. The image of $\mathcal{C}$ under Q is an oblique cylinder $\mathcal{C}_\alpha$, i.e., the strip bounded by the lines $v=\pm\pi-u/k$. We define the web map "modulo $\mathcal{C}_\alpha$" as

$$\tilde{\mathbf{\Phi}}_{\rm w}=\mathbf{\Phi}_{\rm w}\ \mathrm{mod}\ \mathcal{C}_\alpha\colon\ \mathbf{w}_{n+1}=A\cdot[\mathbf{w}_n+\mathbf{F}(\mathbf{w}_n)]-m\tilde{\mathbf{w}}, \tag{6}$$

where $\tilde{\mathbf{w}}=Q\cdot(2\pi,0)=(2\pi k,0)$ and m is the unique integer such that $\mathbf{w}_{n+1}\in\mathcal{C}_\alpha$. The following exact relation then holds for all orbits with initial conditions $\mathbf{z}_0\in\mathcal{C}$ (or $\mathbf{w}_0\in\mathcal{C}_\alpha$):

$$\mathbf{\Phi}_{\rm s}^{(K,\kappa)}=\mathbf{\Psi}_{\mathcal{C}}^{(K,\kappa)}=Q^{-1}\circ\tilde{\mathbf{\Phi}}_{\rm w}\circ Q. \tag{7}$$

For integer $K=-3,-2,-1$ [corresponding, by relation (5), to $q\equiv 2\pi/\alpha=3$, 4, 6, respectively], it is easy to show that the orbit structure of $\mathbf{\Psi}^{(K,\kappa)}$ is periodic with unit cell $\mathbb{T}^2=[-\pi,\pi)^2$. This implies a similar periodicity for $\mathbf{\Phi}_{\rm w}=Q\circ\mathbf{\Psi}^{(K,\kappa)}\circ Q^{-1}$ with unit cell $\mathbb{T}^2_\alpha=Q\cdot\mathbb{T}^2$. In fact, $\mathbf{\Phi}_{\rm w}$ has crystalline symmetry (triangular, square, hexagonal for $q=3$, 4, 6, respectively) [8,9]. One can then expect the existence of an extended chaotic orbit having this symmetry and forming a "stochastic web." This web, which has been observed for particular maps $\mathbf{\Phi}_{\rm w}$ [8,9], encircles the torus $\mathbb{T}^2_\alpha$ in two independent directions. This implies global chaos for the map (6) in $\mathcal{C}_\alpha$ and, due to Eq. (7), also for $\mathbf{\Phi}_{\rm s}^{(K,\kappa)}$ in $\mathcal{C}$.

For noninteger K, the maps $\mathbf{\Psi}^{(K,\kappa)}$ and $\mathbf{\Phi}_{\rm w}$ exhibit no periodicity and there is no simple relation between the orbit structures of $\mathbf{\Phi}_{\rm s}^{(K,\kappa)}$ and $\mathbf{\Phi}_{\rm w}$. In the $\kappa=0$ case, theoretical arguments and numerical evidence [6] strongly indicate that for irrational q the torus $\mathbb{T}^2$ can be partitioned into two regions having nonzero area: (a) A connected pseudochaotic region (zero Lyapunov exponent). (b) An apparently dense set of elliptic islands whose boundaries do not cross or touch the discontinuity line $x=-\pi$. Because of the last fact, the pseudochaotic region encircles $\mathbb{T}^2$ in both the x and p directions, implying global pseudochaos in $\mathcal{C}$. This will generally turn into global weak chaos when a small perturbation $\kappa g(x)$ is applied. Figure 1(b) shows an example for $\alpha=\pi(\sqrt{5}-1)/2$ ($K\approx-2.7247$) and $\kappa=0.15$.

Accelerator-mode fixed points (AFPs) of map (1) satisfy $p_1-p_0=2\pi j$ and $x_1=x_0=x_1-p_1+2\pi j'$ for integers $j\neq 0$ and j'. One can choose $p_0=0$ and, for $\mathbf{\Phi}_{\rm s}^{(K,0)}$ ($\kappa=0$), we get $x_0=2\pi j/K$. Since $x_0\in(-\pi,\pi)$, one must have $j=\pm 1$ and $-4<K<-2$. The latter results remain essentially unchanged for sufficiently small κ. The AFPs are surrounded by relatively large AIs (see Fig. 1) and a strong superdiffusion (large μ) was always observed numerically for $-4<K<-2$. In what follows, we shall study in detail the case of $K=-3$ with $g(x)=\sin x$ on the basis of relation (7). Figure 2 shows the stochastic web of $\mathbf{\Phi}_{\rm w}$ ($q=3$) for $\kappa=0.8$. The "cylinder" $\mathcal{C}_\alpha$ is the oblique strip bounded by the parallel dashed lines. Together with these lines, the two horizontal dashed segments define the unit cell $\mathbb{T}^2_\alpha$ in which there appears, up to the transformation Q in Eq. (7), the chaotic region in Fig. 1(a). The jth unit cell in $\mathcal{C}_\alpha$, $j=-\infty,\ldots,\infty$, contains one "hexagonal" island H_j and two "triangular" islands, L_j and R_j. The hyperbolic (x) points *a*, *b*, *d*, and *e* lie on the boundaries of $\mathcal{C}_\alpha$ while *c* and *f* are inside $\mathcal{C}_\alpha$. The points *a*, *b*, *c* are equivalent, modulo $\mathbb{T}^2_\alpha$, to *d*, *e*, *f*, respectively. It is interesting to see first how the AFPs emerge according to (7). The islands H_j, L_j, R_j are invariant under $\mathbf{\Phi}_{\rm w}^3$ and their centers CH_j, CL_j, CR_j are fixed points of $\mathbf{\Phi}_{\rm w}^3$ which are rotated clockwise by $\alpha=2\pi/3$ under $\mathbf{\Phi}_{\rm w}$. Then, denoting $\mathbf{\Phi}_{\rm w}$ by $\mapsto$ and modulo $\mathcal{C}_\alpha$ by $\Rightarrow$, it is clear from Fig. 2 that $\mathrm{CL}_{-1}\mapsto\mathrm{CL}_0\mapsto\mathrm{CL}_0'\Rightarrow\mathrm{CL}_1\mapsto\mathrm{CL}_1'\Rightarrow\mathrm{CL}_2$. In general, we see that $\tilde{\mathbf{\Phi}}_{\rm w}(\mathrm{CH}_j)=\mathrm{CH}_j$, $\tilde{\mathbf{\Phi}}_{\rm w}(\mathrm{CL}_j)=\mathrm{CL}_{j+1}$, and $\tilde{\mathbf{\Phi}}_{\rm w}(\mathrm{CR}_j)=\mathrm{CR}_{j-1}$, so that CL_j and CR_j correspond to the AFPs and L_j and R_j correspond to the AIs.

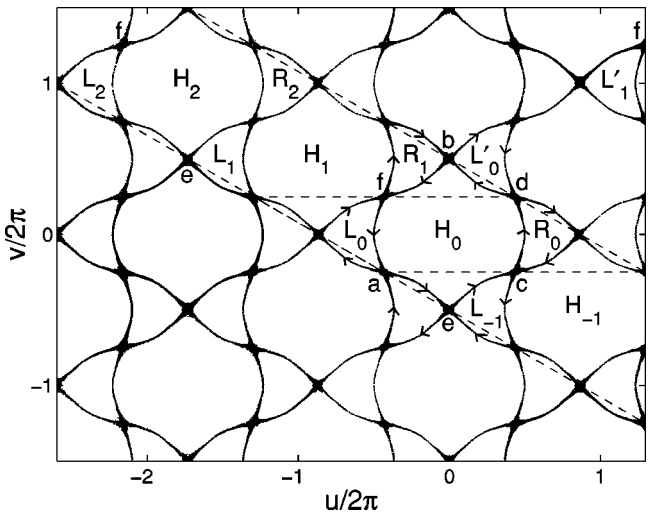

FIG. 2. Stochastic web of the web map $\mathbf{\Phi}_{\rm w}$ related by Eq. (7) to the standard map defined in the caption of Fig. 1(a). See text for details.

Extensive numerical observations indicate that for small κ a chaotic orbit is always a random sequence of three types of motion: (a) A "H motion," bounded in p, sticking around the boundary of H_j. (b) A "flight" in the positive or (c) negative p direction, accompanied by stickiness to the boundary of L_j or R_j, respectively. Remarkably, a flight was always found to be a quasiregular *sequence of steps*. An example of such a flight, interrupted by a H motion, is shown in Fig. 3 for $\kappa=0.3$. Very long, uninterrupted flights (of at least 10^6 iterations) were usually observed for $\kappa\leqslant 0.3$. The steps in the flights clearly leave their fingerprints in the strong superdiffusion of $\langle p_n^2/2\rangle$, at least for small n (see inset in Fig. 3).

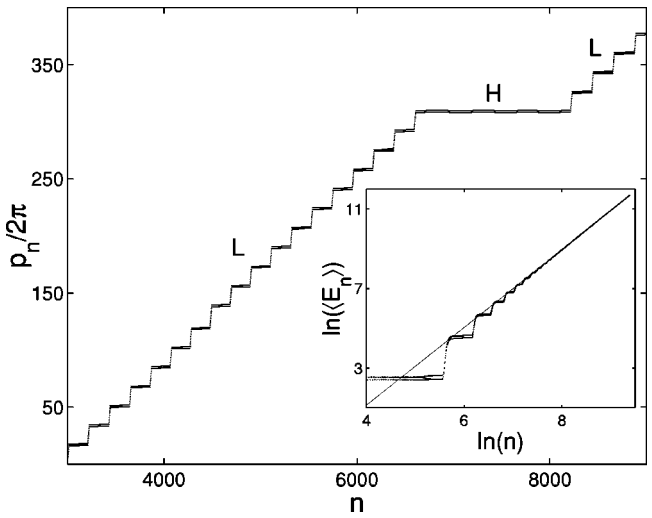

FIG. 3. Chaotic flight, interrupted by a H motion, for $K=-3$, $\kappa=0.3$, and $g(x)=\sin x$. The inset shows $\ln(\langle E_n \rangle)$ vs $\ln(n)$ (dotted line), where $E_n=p_n^2/2$, the average $\langle\ \rangle$ is over an ensemble of 10^6 initial conditions well localized around $(x=0,\ p=-\pi)$, and $n_{\max}=12\,000$; the linear fit (solid line) has slope $\mu\approx 1.96$.

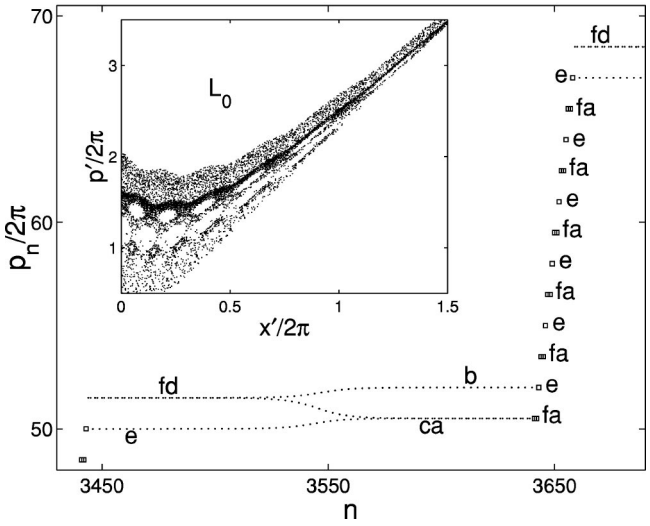

FIG. 4. Magnification of one step in the chaotic flight shown in Fig. 3. The horizontal part of the step (dots) consists of efd cycles followed by cab cycles (total of 198 points). The vertical part (squares) consists of six acceleration cycles fae (18 points). The inset shows the acceleration spot $\{a(\mathrm{L}_0)\}$ in unit cell $j=0$ using the variables $x'=(x+\pi)\times 10^5$ and $p'=(p+\pi)\times 10^5$.

This steplike structure will now be explained using relation (7). The notation $a(\mathrm{L}_j)$ (and similar notation for other x points and islands) will indicate a web (chaotic) point sticking to the L_j boundary very close to *a* and *inside* $\mathcal{C}_\alpha$; if this point is *outside* $\mathcal{C}_\alpha$, it will be denoted by $\overline{a}(\mathrm{L}_j)$. For small $\kappa>0$, $\mathbf{\Phi}_{\mathrm{w}}$ is almost a clockwise rotation by $\alpha=2\pi/3$ while the motion of web points under $\mathbf{\Phi}_{\mathrm{w}}^3$ is a slow drift in the directions of the stable and unstable manifolds, indicated by arrows in Fig. 2. Since the drift velocity vanishes near x points, a cycle such as $e(\mathrm{L}_{-1})\mapsto f(\mathrm{L}_0)\mapsto d(\mathrm{L}_0')$ can repeat many times. This cycle will then drift to the cycle $c(\mathrm{L}_{-1})\mapsto a(\mathrm{L}_0)\mapsto b(\mathrm{L}_0')$ which can also repeat many times. The cycles efd and cab give the "horizontal" part of a step, where *p* is bounded around its values at the x points (see Fig. 4). This part contains *l* cycles ($l=66$ in Fig. 4), where *l* is the largest integer such that all points $\mathbf{\Phi}_{\mathrm{w}}^i[e(\mathrm{L}_{-1})]$, $i=0,\ldots,3l-1$, lie *inside* $\mathcal{C}_\alpha$, so that no modulo $\mathcal{C}_\alpha$ has to be taken in the cycles. The "vertical" part of a step is due to the following process. The last cab cycle is followed by the cycle $c(\mathrm{L}_{-1})\mapsto a(\mathrm{L}_0)\mapsto \overline{b}(\mathrm{L}_0')$, where $\overline{b}(\mathrm{L}_0')$ is *outside* $\mathcal{C}_\alpha$. Taking then the modulo $\mathcal{C}_\alpha$, $\overline{b}(\mathrm{L}_0')\Rightarrow e(\mathrm{L}_1)$, we see that $a(\mathrm{L}_0)$ is mapped into $e(\mathrm{L}_1)$ by $\tilde{\mathbf{\Phi}}_{\mathrm{w}}$. Next, $\tilde{\mathbf{\Phi}}_{\mathrm{w}}[e(\mathrm{L}_1)]=f(\mathrm{L}_2)$. Thus, since *c* is equivalent to *f*, the cycle cae is actually an "acceleration" cycle fae with $\tilde{\mathbf{\Phi}}_{\mathrm{w}}^3[f(\mathrm{L}_{-1})]=f(\mathrm{L}_2)$. The set $\{a(\mathrm{L}_0)\}$ of all points $a(\mathrm{L}_0)$ which are mapped into points $\overline{b}(\mathrm{L}_0')$ by $\mathbf{\Phi}_{\mathrm{w}}$ is the *acceleration spot* (AS) in unit cell $j=0$. As shown by the inset in Fig. 4, the AS touches the line $x=-\pi$ $(x'=0)$, corresponding to the lower boundary of $\mathcal{C}_\alpha$. The cycle fae will repeat *r* times ($r=6$ in Fig. 4), where *r* is the largest integer such that all points $\tilde{\mathbf{\Phi}}_{\mathrm{w}}[f(\mathrm{L}_{3i-1})]$ mod $\mathbb{T}_\alpha^2$, $i=0,\ldots,r-1$, lie in the AS. After *r* fae cycles, one leaves the AS by crossing the line $x=-\pi$ and arrives to $\overline{a}(\mathrm{L}_0)$ which is equivalent to $d(\mathrm{L}_0')$. Thus, $\tilde{\mathbf{\Phi}}_{\mathrm{w}}[f(\mathrm{L}_{3r-1})]$ is equivalent to $d(\mathrm{L}_0')$, *not* to $a(\mathrm{L}_0)$. The horizontal efd cycles of the next step then start. This completes the analysis of one step.

Figure 4 shows a strong trapping near six islands in the AS. In fact, by considering a large number of steps in very long orbits, we found that *r* assumes only two values for $\kappa=0.3$: $r=6$ with probability $P\approx 0.95$ and $r=7$ with $P\approx 0.05$. The value of *l* ranges between $l=53$ and $l=82$. This range should be associated with the continuation of the trapping, outside the AS, near the island chain to which the six AS islands belong. As κ decreases, the steplike structure of the flights becomes more pronounced and the high regularity of the vertical parts of the steps, i.e., the values of *r*, continues to be observed. For $\kappa=0.2$, $l=88-136$ and $r=11$ ($P\approx 0.99$) or $r=12$ ($P\approx 0.01$). For $\kappa=0.1$, $l=150-259$ and $r=29$ ($P\approx 0.93$) or $r=30$ ($P\approx 0.07$).

In conclusion, our study of the $K=-3$ case indicates that the global superdiffusion of weak chaos is basically different in nature from the superdiffusion observed in the usual standard and web maps [3,5]. In the latter systems, the AIs are *"tangle"* islands [4]. These islands born in a strong-chaos regime and are fundamentally different from normal islands, e.g., resonance or web islands, which continue to exist in an integrable limit. Since a tangle island lies inside the lobe of a turnstile [4], it causes the acceleration of chaotic orbits sticking *all around* its boundary. On the other hand, relation (7) implies that the AIs for $K=-3$ are essentially normal web islands folded back into the cylinder. As a consequence, one can have a situation that a chaotic orbit sticking to the AI boundary is accelerated *only* at tiny acceleration spots, in sharp contrast with the case of tangle islands. The resulting steplike structure of the chaotic flights is gradually assumed also by elliptic flights with initial conditions approaching the AI boundary from inside the AI. The basic origin of both the

AIs and the acceleration spots is the folding-back mechanism. Quantum manifestations of the superdiffusion in the usual standard map are well known [10,11] and have been observed in experimental realizations of the quantum kicked rotor [12]. The perturbed sawtooth map (1) with Eq. (2) corresponds to a kicked rotor with a nonsmooth potential. The quantum version of such a system is experimentally realizable by, e.g., an optical analogue [13]. It should be then interesting to study the fingerprints of the new kind of superdiffusion in the corresponding quantum systems. Quite recently [14,15], the quantum sawtooth map was found to be a suitable model for quantum computation of complex dynamics. The exponential-decay rate of the concurrence (measure of quantum entanglement) was shown to be proportional to the classical diffusion coefficient [15]. The extension of this study to the perturbed sawtooth map, with its new kind of chaotic-transport properties, thus appears to be a natural and interesting future task.

This work was partially supported by the Israel Science Foundation administered by the Israel Academy of Sciences and Humanities.

[1] B.V. Chirikov, Phys. Rep. **52**, 263 (1979).
[2] J.M. Greene, J. Math. Phys. **20**, 1183 (1979).
[3] R. Ishizaki, T. Horita, T. Kobayashi, and H. Mori, Prog. Theor. Phys. **85**, 1013 (1991).
[4] V. Rom-Kedar and G. Zaslavsky, Chaos **9**, 697 (1999).
[5] G.M. Zaslavsky, Phys. Rep. **371**, 461 (2002), and references therein.
[6] P. Ashwin, Phys. Lett. A **232**, 409 (1997).
[7] J.R. Cary and J.D. Meiss, Phys. Rev. A **24**, 2664 (1981).
[8] G.M. Zaslavsky, R.Z. Sagdeev, D.A. Usikov, and A.A. Chernikov, *Weak Chaos and Quasi-Regular Patterns* (Cambridge University Press, Cambridge, 1991), and references therein.
[9] I. Dana and M. Amit, Phys. Rev. E **51**, R2731 (1995).
[10] B. Sundaram and G.M. Zaslavsky, Phys. Rev. E **59**, 7231 (1999).
[11] A. Iomin, S. Fishman, and G.M. Zaslavsky, Phys. Rev. E **65**, 036215 (2002).
[12] B.G. Klappauf, W.H. Oskay, D.A. Steck, and M.G. Raizen, Phys. Rev. Lett. **81**, 4044 (1998).
[13] J. Krug, Phys. Rev. Lett. **59**, 2133 (1987).
[14] G. Benenti, G. Casati, S. Montangero, and D.L. Shepelyansky, Phys. Rev. Lett. **87**, 227901 (2001); Eur. Phys. J. D **22**, 285 (2003).
[15] S. Bettelli and D.L. Shepelyansky, Phys. Rev. A **67**, 054303 (2003).